Biofabrication of copper oxide nanoparticles mediated with Echium amoenum petal extract for evaluation of biological functions

Article *in* Biomass Conversion and Biorefinery · September 2023

DOI: 10.1007/s13399-023-04796-4

CITATIONS
0

READS
57

9 authors, including:

Pegah Shakib
Lorestan University of Medical Sciences
77 PUBLICATIONS **295** CITATIONS
SEE PROFILE

Sarah Alsallameh
Gilgamesh Ahliya University Gau
14 PUBLICATIONS **0** CITATIONS
SEE PROFILE

A. Marzban
Lorestan University of Medical Sciences
80 PUBLICATIONS **555** CITATIONS
SEE PROFILE

Biomass Conversion and Biorefinery
https://doi.org/10.1007/s13399-023-04796-4

ORIGINAL ARTICLE

Biofabrication of copper oxide nanoparticles mediated with *Echium amoenum* petal extract for evaluation of biological functions

Pegah Shakib[1] · Seyedeh Zahra Mirzaei[2] · Zeinab Sharafi[1] · Reza Saki[3] · Gholam Reza Goudarzi[1] · Asghar Sepeavand[1] · Sarah Alsallameh[4] · Hamed Esmaeil Lashgarian[1] · Abdolrazagh Marzban[1]

Received: 25 April 2023 / Revised: 12 August 2023 / Accepted: 23 August 2023

Abstract

In this study, *Echium amoenum* (known as borage) petals, popular as a medicinal herb, was used for producing copper nanoparticles (CuO NPs) for the first time. Since borage metabolites are bioactive, they were used as bioreductive agents for synthesizing CuO NPs. For this, phytochemical compositions of EA extract were analyzed qualitatively before fabricating CuO NPs. Various measurements were conducted to characterize the CuO NPs, including UV–vis, FTIR, SEM–EDS, TEM, XRD, DLS, and the zeta potential. Additionally, EA-CuO NPs were examined for antimicrobial, free radical scavenging and cytotoxic activities. The surface plasmon resonance peak of the EA-CuO NPs was identified as 346.6 nm based on UV–visible spectroscopy. FTIR spectra proposed possible functional groups associated with EA-CuO NP formation. According to the SEM and TEM images, the EA-CuO NPs were spherical and ranged from 30 to 40 nm. The crystallites were estimated to be particulate at 28.5 nm in size, with the copper-to-oxygen ratio of 60.16:24.96 determined by XRD and EDX. There was an approximate IC_{50} value of 35.46 µg/ml for the DPPH and 70.11 µg/ml for the H_2O_2 scavenging activity of EA-CuO NPs. A MIC value of 80 µg/ml was obtained for EA-CuO NPs against *Staphylococcus aureus*, *Staphylococcus saprophytic*, and *Klebsiella pneumonia*. However, MIC values for EA-CuO NPs against *Pseudomonas aeruginosa* and *Candida* species were 160 and 600 µg/ml, respectively. Based on the findings, EA-CuO nanoparticles have the potential to be used as an alternative to antibiotics to treat antibiotic-resistant pathogens. Given this, it would be prudent to conduct detailed studies into the mechanism of action and side effects of EA-CuO NPs before they are applied as antimicrobial agents for therapeutic purposes.

Keywords Biogenic CuO NPs · Antibacterial activity · Antifungal activity · Antioxidant capacity · *Echium amoenum*

1 Introduction

Recent studies have found that most common antimicrobial compounds are no longer effective against at least some bacteria due to increasing antibiotic resistance [1]. Nanotechnology is a new research area recently introduced to medicine and treatment. Though nanotechnology has been able to solve many problems in various sciences, concerns exist regarding their host toxicity and environmental challenges in medical sciences. Since metal NPs are widely distributed throughout the environment and cause poisoning when consumed or exposed to living organisms, various research efforts have been conducted to improve their properties, reduce their toxicity, and increase their biocompatibility [2]. Even with some limitations, metal nanoparticles are still promising therapeutic agents, especially for cancers and other drug-resistant diseases. Currently, scientists are developing alternatives to synthesizing metal NPs that reduce their toxicity and improve their consumption. Many scientists are currently looking into the possibility of engineering green NPs by bioactive molecules and living organisms. Various metal NPs with favorable biological properties have been synthesized using polysaccharides, fatty acids, proteins, nucleic acids, and other biomolecules [3, 4].

✉ Abdolrazagh Marzban
marzban86@gmail.com

[1] Razi Herbal Medicines Research Center, Lorestan University of Medical Sciences, Khorramabad 6816968773, Iran

[2] Medical Biology Research Center, Health Technology Institute, Kermanshah University of Medical Sciences (KUMS), Kermanshah 6714415185, Iran

[3] Department of Microbiology, Kermanshah University of Medical Sciences (KUMS), Kermanshah 6814869914, Iran

[4] Department of Medical Laboratories Techniques, College of Health and Medical Techniques, Gilgamesh Ahliya University Gau, 10022 Baghdad, Iraq

Cu and CuO NPs are applied in many industries, including textiles, paints, and agriculture, due to their moderate toxicity, favorable stability, and cost-effective production. Several studies have demonstrated that CuO NPs have promising antimicrobial, antioxidant, antiviral, and anticancer properties [3]. Cu-based NPs can be produced physically, chemically, or biologically depending on the intended purpose. Therefore, the properties of the desired products must be considered [5]. CuO NPs with biological applications can be fabricated using various techniques, including combinations of biological and non-biological approaches. Exploiting plant bioactive compounds to prepare Cu NPs with therapeutic and medicinal potential is an intriguing opportunity. In the meantime, medicinal plants are effective because they are non-toxic, and their metabolites are known to have medical properties.

E. amoenum is an annual plant in the family Boraginaceae, *Echium* genus. It is considered one of the most important herbal medicines in traditional Iranian medicine. Several bioactive compounds have been found in the purple-blue petals of *E. amoenum*, including polyphenols, anthocyanins, glucosides, and others [7]. These compounds are known for their health-promoting properties [8, 9]. There is a high reducing capacity in the metabolites of *E. amoenum* that allows them to form and stabilize metal NPs [10]. It has been demonstrated that copper, silver, gold, zinc, selenium, and iron NPs can be synthesized biologically using the metabolites of *E. amoenum* [6].

This study aims to produce biogenic CuO NPs by using the hydroalcoholic extract of *E. amoenum* as a reducing and capping agent. Afterward, CuO NPs were investigated for their antimicrobial, antioxidant and cytotoxic activities.

2 Experimental

2.1 Chemicals and reagents

MTT reagent ((3-(4,5-dimethylthiazol-2-yl)-2,5-diphenyltetrazolium bromide), crystal violet, and Folin–Ciocâlteu reagents were purchased from Sigma Aldrich chemical company. $CuSO_4{\cdot}5H_2O$, H_2SO_4, and $BaCO_3$ were provided by Merck Chemical Co. (Germany, USA). All other chemicals were laboratory-quality as received. The standard bacterial strains, including methicillin-resistant *Staphylococcus aureus*, MRSA (ATCC 33591), *Klebsiella pneumoniae* (ATCC 700603), and *Staphylococcus saprophyticus* (ATCC 6538P) and multidrug-resistant *Pseudomonas aeruginosa* (Clinical isolate), *Candida glabrata* (ATCC 90030), and *Candida albicans* (ATCC 10231), were provided from a microorganism culture collection by the Iranian Research Organization for Science and Technology (IROST), Tehran, Iran. The KB cell line was sourced by the cell bank of the Tehran Pasteur institute, Tehran, Iran.

2.2 Plant sample preparation and ethanol extraction

The petals of *E. amoenum* were collected from the Khorramabad Mountain area (Lorestan, Iran). The petals were washed with deionized water and dried in the dark for 10 days. After that, 5 g of the dried petals was extracted in 100 mL of ethanol under incubation conditions at 45 °C by a bath-sonication. After 6 h, the ethanol extract of *E. amoenum* (EA extract) was passed through a Whatman filter paper. The filtrate of EA extract was used to synthesize CuO NPs and phytochemical studies.

2.3 Qualitative phytochemical Analysis of EA extract

2.3.1 Total phenolic and flavonoid contents

Total phenols in the *E. amoenum* petal extract were determined using the Folin-Ciocalteu (FC) colorimetric method. Briefly, 1.0 mg of EA (ethanol solution) was mixed into 3 mL of 10% (V/V) FC reagent and 1.0 ml of Na_2CO_3 (5%, W/V). The sample was then vortexed for 30 min and incubated for 15 min at 45 °C. Assays of total flavonoids were conducted by adding methanol solutions of $Al(NO_3)_3$ (10% W/V) and $Pb(C_2H_3O_2)_2$ (0.1% W/V) to EA extract. The change in color of the reaction solution showed that flavonoids were present in the extract [11].

2.3.2 Total tannin content

The total tannin content in the EA extract was confirmed using the $FeCl_3$ reagent. The appearance of blue or green colors usually indicates the presence of condensed or hydrolyzed tannins [12].

2.3.3 Total saponin content

The saponin content of the EA extract was determined by adding 10 mg of the extract to 10 ml of deionized water. Saponins were detected by forming a foam layer over the solution after shaking vigorously [12].

2.3.4 Total alkaloid assay

The alkaloids in the EA extract were detected using Hager's reagent. Picric acid (1%) and EA extract in a ratio of 2:1 were mixed in a glass container. The presence of alkaloids in the EA extract was demonstrated by forming a yellow precipitate in the sample [12].

Journal : Large 13399 | Article No : 4796 | Pages : 11 | MS Code : 4796 | Dispatch : 29-8-2023

2.3.5 Total terpenoid assay

Five milliliters of EA extract was added to 2 ml chloroform in a 10-ml glass tube. Afterward, 3 ml of H_2SO_4 (98%) was gently added to the reaction sample and allowed to react. After a few min, terpenoids were detected by forming a reddish-brown ring interface in the reaction solution [13].

2.3.6 Total steroidal glycoside

The presence of glycosides was evaluated using two different methods. In the first method, 2.0 ml of acetic acid (glacial) was mixed with 2.0 ml of chloroform and added to 2.0 ml of EA extract. In the meantime, the mixture was cooled, and then 1 ml of H_2SO_4 (98%) was added. The appearance of green color indicates glycan aglycone steroidal glycoside in the reaction sample [13]. For the second method, 2.5 ml of glacial acetic acid was mixed with 0.5 ml of $FeCl_3$ solution (1% W/V) and then added to 5 ml of EA extract. The formation of a brown ring has been attributed to cardiac steroidal glycosides after adding 1 ml of H_2SO_4 [12].

2.4 Biosynthesis of CuO NPs by EA extract

In this study, CuO-NPs were fabricated using ethanol extract of EA as a capping and reducing agent following a hydrothermal process described by Prakash et al. (2021) under optimal conditions [14]. In a 250-ml flask, 20 ml of EA extract was dissolved in 40 ml deionized water (DW). Forty milliliters of $CuSO_4{\cdot}5H_2O$ (3 mM) solution was added to the EA extract while stirring on a magnetic hot plate at 65 °C. Changing the color of the reaction sample from blue to brownish-red implied the formation of EA-CuO NPs. Additionally, the formation of EA-CuO NPs was monitored using a UV–visible spectrophotometer (Jenway UV–vis model 6505, UK) at 200–800 nm. The EA-CuO NPs were then precipitated using centrifugation at 14,000 rpm at 4 °C for 15 min. To dry the pellets, they were first washed twice in DW and then placed in an oven at 100 °C.

2.5 Characterization of biogenic CuO-NPs

The physicochemical characteristics of EA-CuO NPs were examined using the following analytical methods.

FTIR spectroscopy was used to investigate possible functional groups in biogenic CuO NPs. For this purpose, EA-CuO NP powder was mixed with KBr and filled into discs at high pressure. The FTIR spectrum was recorded on an FTIR spectrophotometer (FS 66/s, Bruker Optics, Billerica, MA) over a scanning range of 400–4000 cm^{-1}. FE-SEM imaging and energy-dispersive X-ray analysis (MIRA3, TESCAN, Czech Republic) were performed to analyze the morphology and elemental composition. ImageJ Ver.2 (NIH, USA) software was used to calculate particle size distributions from SEM images. TEM image was taken on Philips EM 208S (Netherlands). X-ray powder diffraction analysis was conducted using an X-ray diffractometer (Bruker, D8 Advance, Germany) equipped with Cu K radiation of 0.15418 nm at 30 kV and 15 mA applying a scanning rate of 0.4°/min from 10 to 80°. The crystallite size and phase type of EA-CuO NPs were calculated using XPert HighScore Plus software Ver.2.2.

2.6 Antimicrobial assay

The antimicrobial activity of EA-CuO NPs was evaluated by well-diffusion agar (WDA). In the 8-cm diameter bacterial culture plates, 4 wells were created using a sterile punch. Then, fresh bacterial cells were lawn on agar plates using a sterile cotton swab. Thirty microliters of different concentrations of EA-CuO NPs (25, 50, 100, and 200 µg/ml) were separately poured into the wells. The plates were incubated at 37 °C for 24 h to appear growth inhibition zones. Microdilution method was used to determine the minimum inhibitory concentration (MIC). This experiment was conducted in a 96-well microplate in which 35 µl dilutions of EA-CuO NPs (0–200 µg/ml) were added to 65 µl of MHB culture media containing 0.5 McFarland densities (1.5×10^8 CFU/ml) of bacterial cells. MIC values were determined by measuring the optical density of bacteria at 600 nm after 24 h of incubation at 37 °C. Based on the MIC values, minimum bactericidal concentrations were also calculated [15].

2.7 DPPH scavenging assay

DPPH scavenging was used to determine the antioxidant capacity of EA-CuO NPs and EA extract. For this purpose, various concentrations of EA-CuO NPs or EA extract were added to the DPPH reagent (0.15 mM in methanol). The mixtures were placed in darkness for 30 min to allow the reaction to complete. The ascorbic acid (AA) served as a positive control. The scavenging efficacy of DPPH was calculated using the following Eq. (1):

$$\text{Scavenging efficacy}(\%) = \frac{\text{Blank (A0)} - \text{Sample (A)}}{\text{Blank (A0)}} \times 100 \quad (1)$$

2.8 Cytotoxicity assay of CuO-NPs

Human epidermal nasopharyngeal carcinoma (KB cell line) was used for toxicity assessment of EA-CuO-NPs and EA extract. EA-CuO NPs and EA extract cytotoxicity was examined using different concentrations (0–500 µg/ml). Cells were seeded in T-25 SPL culture flasks containing 5 ml of DMEM

supplemented with 10% FBS until 70% confluence was achieved. Afterward, treatments were conducted in 96-well plates on 10^4 cells in each well and incubation was done for 24 h under standard conditions. The cell viability was determined by adding 10 µl of MTT reagent to cell-grown wells and the plate was incubated for 4 h. Then, 100 µl of DMSO was slowly pipetted into each well. Finally, the sample absorbance was measured at 520 nm using an ELISA reader. Cell viability was calculated as a percentage compared with untreated cells (negative control).

2.9 Statistical analysis

All experiments were conducted in triplicate and at least three times. The results are presented as the means and standard deviations (SD). Cell viability was compared between control (untreated) and treated groups using a one-way analysis of variance with a 95% confidence interval.

3 Results and discussion

3.1 Qualitative analysis of EA phytochemicals

Colorimetric analysis was employed to identify phytochemical compounds in EA extract. As shown in Table 1, phenolics, flavonoids, tannins, alkaloids, aglycone steroidal glycosides, and terpenoids were identified in the EA extract. Numerous studies have previously established that *E. amoenum* contains major bioactive metabolites such as rosmarinic acid, naphthoquinone, flavonoids, anthocyanins, tannins, alkaloids, steroidal glycosides, and terpenoids [7–9, 16]. Additionally, bioactive metabolites responsible for synthesizing the most NPs include polyphenols, flavonoids, alkaloids, tannins, and reducing sugars [10, 17, 18]. Consequently, EA-CuO NPs synthesized by EA extract have a high bioactivity that can be attributed to several active metabolites that act on the NPs to reduce/cap and stabilize them.

3.2 Biosynthesis of EA-CuO NPs by EA extract

EA-CuO NPs were biologically synthesized using EA extract metabolites as reducing and capping agents. Upon adding the EA extract to the $CuSO_4$ solution, the color gradually changed from blue to brownish red due to EA-CuO NP formation (Fig. 1a). Reddish-brown color is attributed to inter-band transitions between Cu electrons in CuO NP structures [19]. According to the findings, the appearance of certain bands at 340–360 nm could be attributed to clusters of [Cu–O–Cu]n in CuO samples [20].

UV–vis spectroscopy demonstrated a typical surface plasmon resonance peak at 346.6 nm (Fig. 1b). As calculated by the Tauc equation, the band gap of EA-CuO NPs was 3.58 eV during direct interband transitions (Fig. 1c). As reported in the literature, there is a direct interband transition at 3.25 eV in bulk CuO and an indirect band gap between 1.0 and 1.7 eV [21]. According to this study, the bandgap of EA-CuO NPs was larger than that of bulk CuO due to the magnitude effect of the NPs. Furthermore, due to the narrow distribution of the particles, it can be assumed that they fall within the nanoscale [22].

3.3 Morphological characterization of EA-CuO NPs

EA-CuO NPs were analyzed using SEM and TEM images to determine their shape and size distribution. As shown in Fig. 2a and b, EA-CuO NPs ranged from 30 to 40 nm, as indicated by the size labels in the SEM image. Although SEM can reveal the surface morphology of NPs, it cannot estimate their size accurately. According to Fig. 2a, regardless of the accumulation of NPs in some regions, they appeared as spheres covered by EA biomolecules. Furthermore, the TEM image confirmed the SEM measurement of NP size and capping (Fig. 2c). In the EDS spectrum of EA-CuO NPs, prominent peaks correspond to Cu at 2.1 and 8.6 keV. The EDS pattern established carbon and oxygen compartments in the backbone of EA-CuO NPs at 0.7 and 1.3 keV, respectively (Fig. 2d). As shown in Fig. 2 e, the size distribution of EA-CuO NPs was determined using both TEM and SEM scaling and ImageJ software to estimate the particle size range. According to this graph, EA-CuO NPs possessed 30–40 nm. In various studies, Cu NPs with biological origins have been demonstrated to have irregular shapes or a variety of nanostructures, including hexagonal, cylindrical, triangular, and prismatic shapes with varying particle sizes based on reducing and capping agents [23, 24].

3.4 FTIR analysis

As seen in Fig. 3 a, the FTIR spectra demonstrated that functional groups in the EA extract metabolites play an

Table 1 Bioactive metabolites present in EA extract based on qualitative assay methods

Total phytochemical	Appearance	Result	Total phytochemical	Appearance	Result
Polyphenol	Blue	Positive	Alkaloid	Red	Positive
Flavonoid	Yellow	Positive	Terpenoid	Reddish-brown	Positive
Tannin	Violet	Positive	Saponin	–	Negative
Cardiac steroidal glycosides	–	Negative	Aglycone steroidal glycoside	Green	Positive

Journal : Large 13399 | Article No : 4796 | Pages : 11 | MS Code : 4796 | Dispatch : 29-8-2023

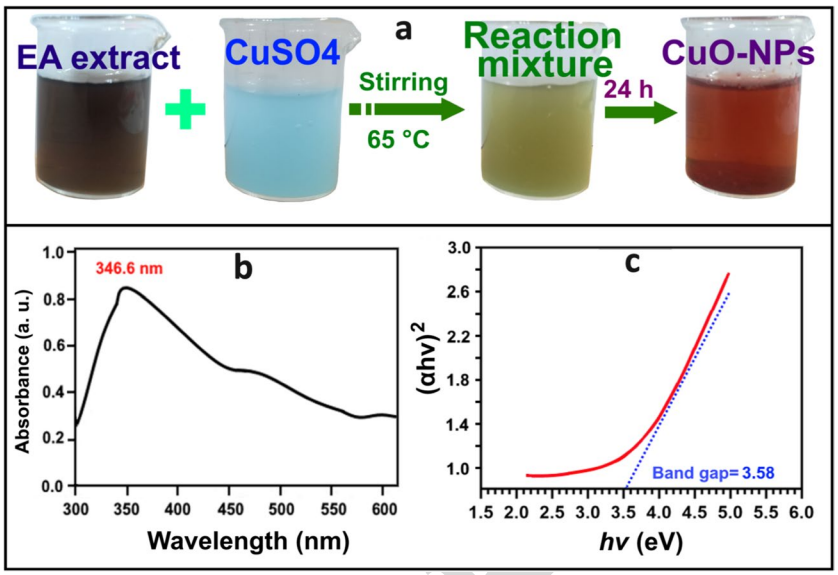

Fig. 1 **a** Color shift of the mixture with the formation of EA-CuO NPs during 24 h, **b** UV–vis spectra of EA-CuO NPs after complete reaction for 24 h and **c** Tauc's plot of the EA-CuO NPs

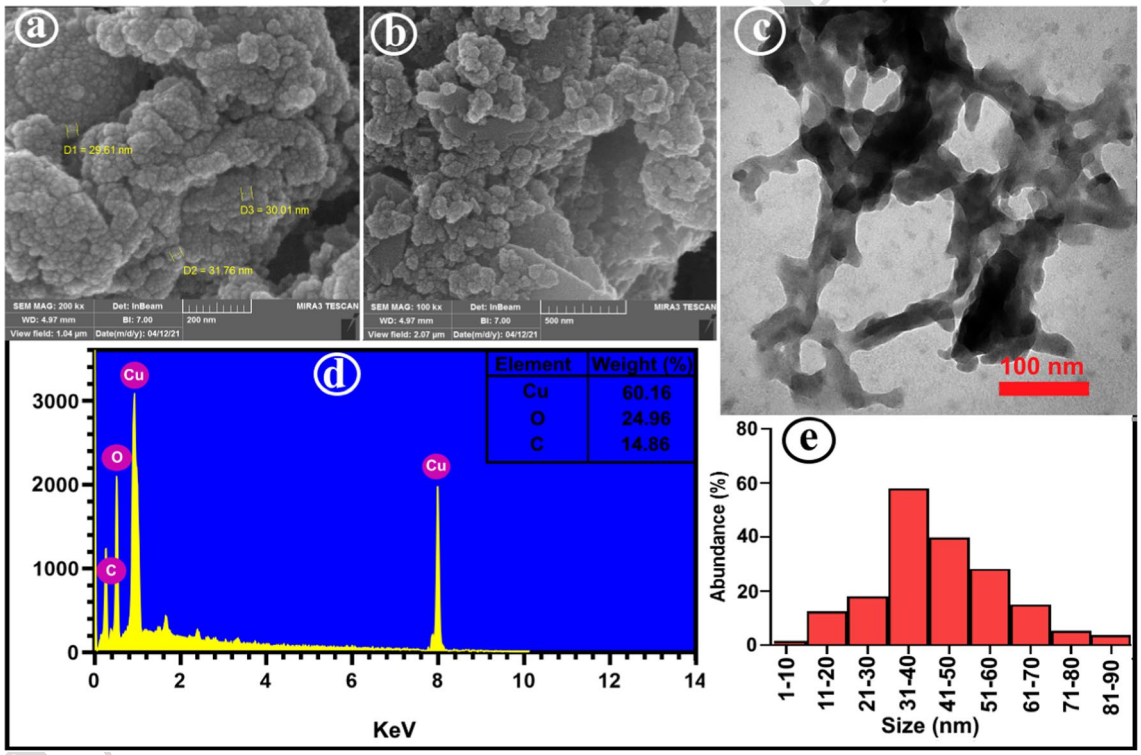

Fig. 2 EA-CuO NP analytics. **a**, **b** TEM image, **c** SEM image, **d** elemental composition analysis (EDX), and **e** Particle size distribution

important role in capping and stabilizing the EA-CuO NPs. An apparent peak at 3349.1 cm^{-1} in the EA extract spectrum was attributed to O–H stretching, which narrowly shifted to 3324.5 cm^{-1} in the EA-CuO NP spectrum [25]. In the EA extract spectrum, peaks at 2965.9 and 2902.2 cm^{-1} are attributed to the CH_2 and CH stretching in the aliphatic backbone [22]. There were significant differences in signal strength for the peaks at 1814.0, 1028.1, and 929.8 cm^{-1} when compared to EA extract, with a few slight shifts (1715.7, 978.9, and 831.5 cm^{-1}) in EA-CuO NP spectrum indicating that polyphenols, carboxylic acids, nitro compounds, and alcohols present in EA extract play an important role in reducing and capping process. The appearance of a stretching peak at 435.5 cm^{-1} is related to Cu–O bonds of EA-CuO NPs that loaded on EA extract [27–29].

Journal : Large 13399 | Article No : 4796 | Pages : 11 | MS Code : 4796 | Dispatch : 29-8-2023

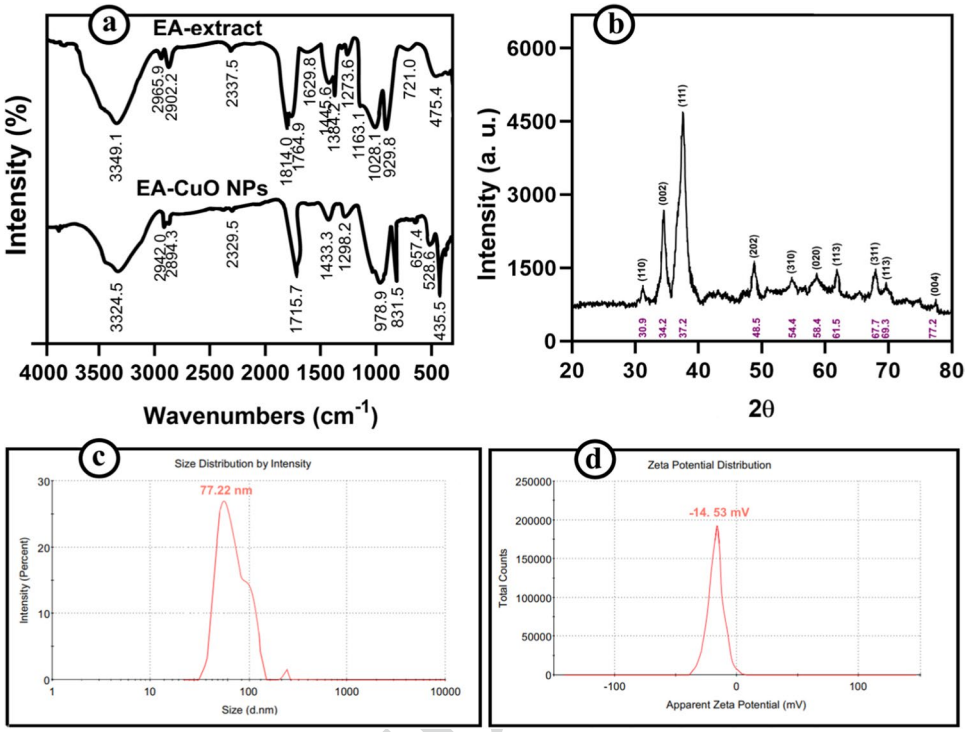

Fig. 3 **a** FTIR spectroscopic pattern of EA-CuO NPs and EA extract, **b** XRD pattern of EA-CuO NPs, **c** particle size distribution of EA-CuO NPs (DLS), and **d** zeta potential of EA-CuO NPs (surface charge) in an aqueous phase

3.5 XRD analysis of EA-CuO NPs

The XRD pattern peaks observed for EA-CuO NPs synthesized by EA extract are shown in Fig. 3b. Intense diffraction peaks at 2Θ angles of 30.9°, 34.2°, 37.2°, 48.5°, 54.4°, 58.4°, 61.5°, 67.7°, 69.3°, and 77.2° correspond to 110, 002, 111, 202, 020, 202, 113, 311, 113, and 004 miller planes, respectively. These diffractions agreed with a typical monoclinic CuO NP nature based on literature [30, 31]. According to the JCPDS standard, EA-CuO NPs showed complete agreement by JCPDS card no. 801268. The crystallite particle size was calculated from an XRD spectrum and was found to be 18.32 nm using Debye–Scherrer's Eq. (2):

$$D = \frac{k\lambda}{\beta Cos\theta} \quad (2)$$

where D is the particle size (nm), k is the Scherrer constant = 0.94, λ represents the X-ray wavelength (1.54060 Å), β is the full-width at half maximum of the peak, and 2 θ is the Bragg's angle.

3.6 Dynamic light scattering and zeta potential analyses

Size distribution (dynamic light scattering) of EA-CuO NPs was measured as hydrodynamic diameters ranged 10–1000 nm as shown in Fig. 3c. The Brownian motion of NPs causes them to scatter the irradiated light at various intensities. Based on the intensity of dispersed light, the zeta average can be calculated for NPs. Accordingly, the zeta average is the maximum intensity of dispersed NPs in hydration form in an aqueous phase [32]. In this study, the zeta average of EA-CuO NPs was determined to be 77.22 nm. As predicted, the zeta average value was greater than NP size calculated by SEM, TEM, and XRD analyses. As seen in Fig. 3d, the zeta potential of EA-CuO NPs was calculated to be − 14.53 mV. In addition, zeta potentials are used to estimate the stability of synthetic nanoparticles by analyzing the attractions and repulsions caused by fluctuations in charge density [30]. Literature indicated that NPs with surface charges outside the range of − 30 mV and + 30 mV exhibit greater electrostatic stability. Meanwhile, bioactive metabolites' role in the stability of NPs was well-established by many studies. Consequently, the presence of capping agents is crucial to prevent the aggregated NPs from forming under physiological conditions [30, 32, 33].

3.7 Antimicrobial activity of EA-Cu NPs

The antibacterial activity of EA-CuO NPs was examined against different bacteria and fungi strains. As seen in Fig. 4, growth inhibition of EA-Cu NPs was determined as dose-dependent modes for all microorganisms. Based on well diffusion agar assay, the maximum inhibition at 200 µg/ml of EA-CuO NPs was found for *K. pneumonia* and then *S. saprophyticus* and *S. aureus* with zone diameters of 30.4, 25.6, and 25.3 mm, respectively. According to Table 2, the MIC values of all treatments were consistent

Journal : Large 13399 | Article No : 4796 | Pages : 11 | MS Code : 4796 | Dispatch : 29-8-2023

with WDA results. In addition, *S. aureus* MRSA was inhibited completely at a MIC value of 80 µg/ml, whereas P. *aeruginosa* was more resistant as compared to other bacterial strains.

Metal NPs have the unique property of having a large surface area relative to their volume, which gives them enhanced reactivity against various pathogens [34]. According to several studies, Cu NPs display antimicrobial activity after attaching to the plasma membrane by generating free reactive oxygen species (ROS) [12, 35]. It has been demonstrated that Cu + ions can readily cross the lipid bilayer and enter the cytosol, leading to the generation of ROS and the oxidation of proteins and lipids. Furthermore, Joseph et al. (2016) suggest that NPs possess a high electrostatic attraction, which results in bacterial cells releasing components [36].

Various factors influence the biological properties of Cu NPs, such as their size, capping agents, and polarity. In many respects,

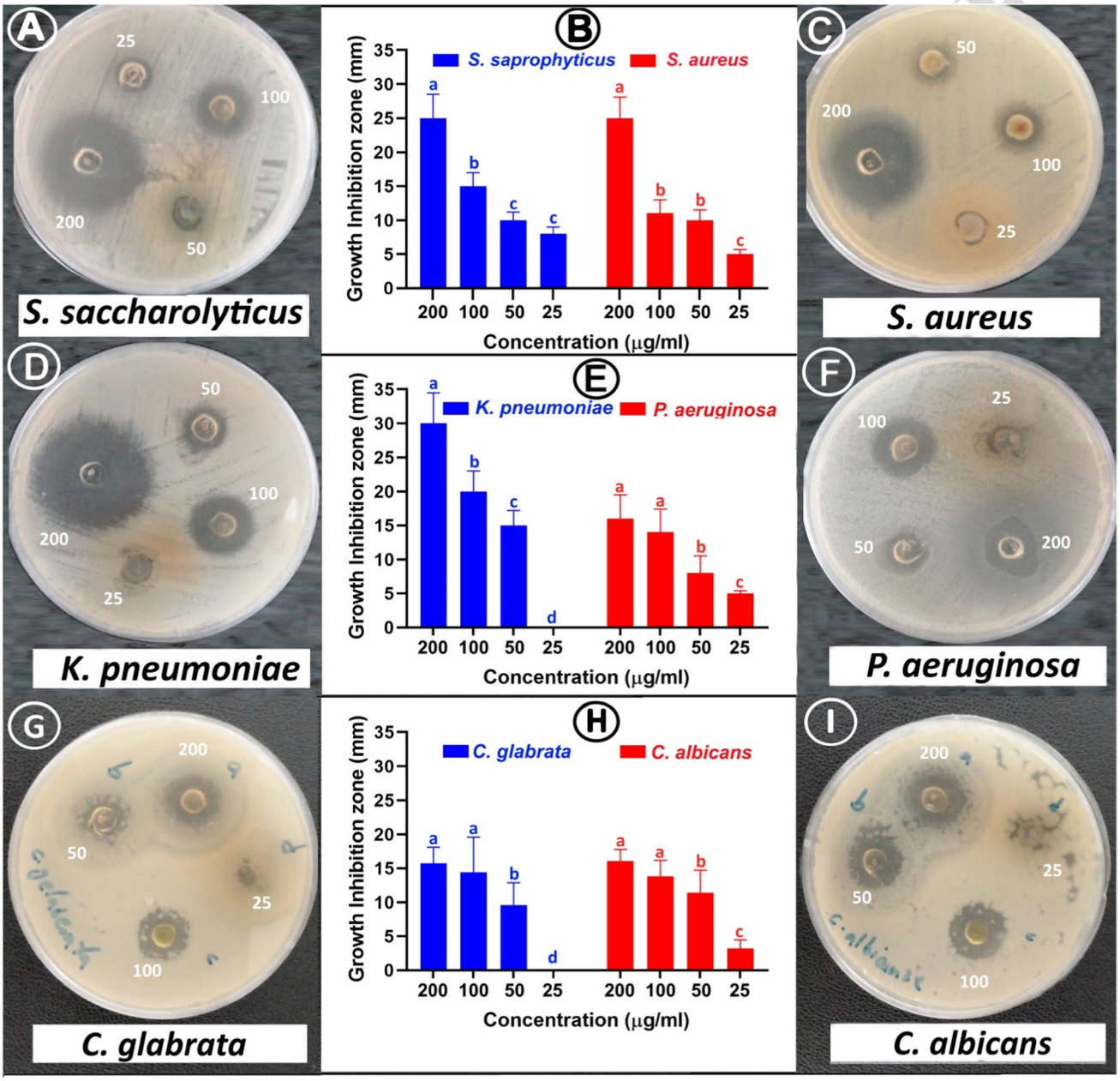

Fig. 4 Antibacterial activity assay of EA-Cu NP antibacterial activity assay of (**a**, **b**, **c**) against *S. aureus* and *S. saprophyticus* (gram-positive bacteria), **d**, **e**, **f** against *K. pneumonia* and *P. aeruginosa* and **g**, **h**, **i** against *C. glabrata* and *C. albicans*. The graphs present zone inhibitions regarding corresponding plates at the right and left sides. The data are presented as mean ± SD from three replicates. Different superscripts display differences between treatements (p-value < 0.05)

Journal : Large 13399 | Article No : 4796 | Pages : 11 | MS Code : 4796 | Dispatch : 29-8-2023

Table 2 Antibacterial performance of EA-Cu NPs: the diameter of growth inhibition zone and MIC for various microorganisms

Microorganism	Concentration (µg/ml)					
	25	50	100	200	Inhibition at MIC	MIC
S. aurous	5.1 ± 0.8	10.4 ± 2.21.0	11.2 ± 2.3	25.6 ± 3.2	11.4 ± 4.1	80
S. saprophyticus	8.5 ± 0.9	10.8 ± 1.0	15.3 ± 2.1	25.3 ± 3.7	13.7 ± 3.8	80
K. pneumoniae	0 ± 0.0	15.4 ± 2.3	20.1 ± 3.4	30.4 ± 5.2	21.1 ± 6.7	80
P. aeruginosa	5.2 ± 0.2	8.3 ± 2.7	14.7 ± 3.6	16.1 ± 4.2	10.6 ± 2.9	160
C. glabrata	0 ± 0.0	9.4 ± 2.5	10.3 ± 3.2	12.5 ± 2.6	28.2 ± 6.1	600
C. albicans	3.1 ± 0.4	11.5 ± 1.3	13.9 ± 2.4	16.1 ± 3.6	31.3 ± 7.0	600

the results of this study are in agreement with those obtained by Punniyakotti et al. (2020) [37]. In their study, Cu NPs synthesized from *Cardiospermum halicacabum* leaf extract had high antimicrobial activity against *P. aeruginosa* (MTCC 424), *E. coli* (MTCC 4296), and *S. aureus* (MTCC 3160). Our study corresponds with previous studies in demonstrating the importance of particle size, which has higher antimicrobial effects at a scale below 100 nm [27]. Furthermore, coating agents also play an active role in biocompatibility and stability within the physiological environment. This study demonstrated the role of biological coatings in Cu NPs' biological activity, which is consistent with other studies. For example, Yugandhar et al. (2018) showed that Cu NPs prepared by *Syzygium alternifolium* plant extract has a synergistic antimicrobial effect with antibiotics. In addition, they reported that the anticancer effect of biological Cu NPs was significantly more effective [32].

Moreover, differences in the antimicrobial potency of NPs can be attributed to bacterial cell structure. The present study found greater antimicrobial effects against Gram-positive bacteria than against Gram-negative bacteria and fungi. This implies that the ability to bind NPs to biomolecules in bacterial cell walls may be crucial. According to Menazea and Ahmed (2020), CuNPs' antimicrobial activity against Gram-positive bacteria may be attributed to their strong binding to carboxyl and amine molecules on bacteria's surfaces [38]. As Kumar et al. (2021) suggested, Cu ions interact with the bacterial genome and disrupt gene expression [39].

Observations revealed that EA-CuO NPs had a weaker antifungal activity than their antibacterial activity, so the treatment dose was increased to 1000 µg to observe fungal inhibition. In this case, the antifungal MIC was determined to be 600 µg/ml (Table 2). According to Poonguzhali et al. (2022), chitosan-coated Cu NPs possess the most antibacterial activity against *Staphylococcus* sp. and *Pseudomonas* sp. and the least antifungal activity against *Candida* sp. and *Aspergillus* sp. [40]. According to their findings, Cu NPs showed greater antifungal activity with increasing doses up to 300 µg/ml. Our results indicate that increasing the dose of EA-CuO NPs inhibited the growth of fungi effectively. Evidence suggests that high-dose treatments could kill fungal strains, but such treatments should be considered restricted in practice because of the cytotoxicity effects of the NPs. In this study, EA-CuO NPs demonstrated increased effectiveness against sensitive and resistant bacterial and fungal pathogens. The studies indicated that Cu NPs might exert different antimicrobial activities against different species of bacteria and fungi depending on the physicochemical properties of the NPs and the type of pathogens.

3.8 Antioxidant capacity of EA-CuNPs

EA-CuO NPs were examined for antioxidant activity based on DPPH scavenging as well as H_2O_2 inhibition measurements in comparison with ascorbic acid (AA) and EA extract. For both assessments, IC_{50} values for EA-CuO NPs, AA, and EA extract were calculated based on concentrations ranging from 0 to 300 µg/ml. DPPH scavenging capacities of EA-CuO NPs, EA extract, and AA were determined to have IC_{50} of 35.46, 37.43, and 95.31 g/ml, respectively (Fig. 5a). As shown in Fig. 5 b, EA-CuO NPs were found to have IC_{50} of 70.11 µg/ml against free H_2O_2. Furthermore, EA extract and AA were inhibited by

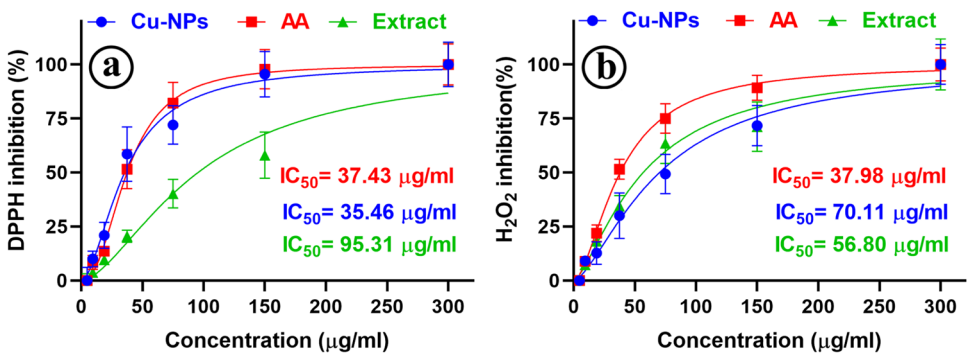

Fig. 5 Antioxidant capacity of EA-CuO NPs. **a** DPPH inhibition activity of EA-CuO NPs compared with EA extract and AA. **b** H_2O_2 inhibition activity of EA-CuO NPs compared with EA extract and AA along with their corresponding IC_{50}

Journal : Large 13399 | Article No : 4796 | Pages : 11 | MS Code : 4796 | Dispatch : 29-8-2023

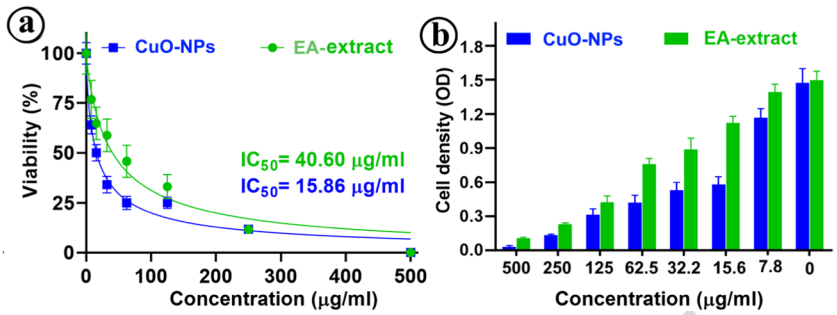

Fig. 6 Cell cytotoxicity assay. **a** Exposure of different concentration of EA-CuO NPs (0–500 µg/ml) on KB cell line based on IC_{50} values and **b** effect of different concentration of EA-CuO NPs (0–500 µg/ml) on the viability based on cell density

H_2O_2 with IC_{50} values of 56.80 and 37.98, respectively. This antioxidant potential of EA-CuO NPs is attributed to their ability to inhibit free radicals, inhibit enzymatic chain reactions, and, most importantly, inhibit hydrogen absorption [41]. The antioxidant properties of nanoparticles are largely attributed to their ability to neutralize free radical oxygen species [34, 42]. The presence of bio-reducing groups in the structure of biogenic NPs has been found to confer substantial antioxidant activity on these molecules [43]. As shown by Rehana et al. (2017), biogenic Cu NPs possess the capability of neutralizing various types of free radicals [42]. According to Din et al. (2017), plant extracts containing flavonoids, polyphenols, sugars, and tannins increased the antioxidant activity of biogenic CuNPs [44].

3.9 Cytotoxicity effects of EA-CuO NPs

EA-CuO NPs were dose-dependently cytotoxic to the KB cell line, so increasing its concentration drastically reduced cell survival. In Fig. 6, EA-CuO NPs exhibited more cytotoxicity than EA extract, so their IC_{50} values were 15.86 and 40.60 µg/ml, respectively. Numerous studies have established that NPs exert their toxicity through a variety of mechanisms, including metabolic as well as structural interactions [39, 45]. Ghasemi et al. (2022) examined the cytotoxicity of biogenic Cu NPs against SW480 Human Colon Cancer Cell Lines. They observed that Cu NPs disrupt the integrity of cell membranes and inhibit metabolic pathways by generating free radicals within cells [46]. Since biogenic nanoparticles are biocompatible, they possess lower toxicity than chemical-based ones and display fewer disruptions to normal cell functions [47]. Although EA-CuO NPs exhibit more toxic properties than EA extract, they may moderate their toxic effects and enhance their biocompatibility [48].

4 Conclusion

In the present study, an attempt was made to synthesize CuO NPs, using petal extract from *E. amoenum* as a reducing and capping agent. The biogenesis of EA-CuO NPs was conducted as anticipated, with favorable properties and bioactivities. According to the physiochemical characteristics, EA-CuO NPs have a spherical shape and are highly pure with a size below 100 nm. According to the results, EA-CuO NPs displayed broad antimicrobial activity against bacterial and fungal strains. However, EA-CuO NPs demonstrated the strongest antibacterial activities against Gram-positive bacteria and weak antifungal activity against fungi. The antioxidant capacity of the EA-CuO NPs was also demonstrated to be satisfactory compared with other reports. Accordingly, this study may provide evidence of the importance of the biological functions of EA extract in capping CuO NPs and improving their bioactivity. Therefore, bioactive therapeutic metabolites, such as flavonoids, polyphenols, and terpenoids, contained in *E. amoenum* extract can affect the behavior of synthesized CuO NPs and their side effects. In our study, we found that EA-CuO NPs have promising bioactivity; however, more extensive trials will be needed to confirm their therapeutic efficacy.

Acknowledgements This research was under potential contribution of Lorestan University of Medical Sciences (LUMS) Vice Chancellor for Research and Technology. The majority of the research was conducted at Razi Herbal Medicines Research Center.

Author contribution Pegah Shakib: conceptualization, visualization, AQ2 and supervision. Seyedeh Zahra Mirzaei: investigation, methodology, original draft. Zeinab Sharafi: conceptualization, methodology. Reza Saki and Gholam Reza Goudarzi: investigation, methodology. Asghar Sepeavand, Sarah Alsallameh, and Hamed Esmaeil Lashgarian: conceptualization, methodology, and supervision. Abdolrazagh Marzban: methodology, supervision, visualization, and writing.

Funding The research project was funded by Lorestan University of Medical Sciences (LUMS) under grant number 1397–1-99–1946.

Data availability All data obtained from experiments were used and analyzed throughout the manuscript.

Declarations

Ethical approval and consent of participation All authors are aware of publication ethics and have consented to publish the manuscript. The ethical committee at LUMS granted permission for this research to be conducted under code: IR.LUMS.REC.1400.

Consent for publication This manuscript has been read and approved by all authors, and it is hereby published in the current format.

Competing interests The authors declare no competing interests.

References

1. Al-Hakkani MF (2020) Biogenic copper nanoparticles and their applications: a review. Appl Sci 2(3):505. https://doi.org/10.1007/s42452-020-2279-1
2. Chauhan N, Thakur N, Kumari A, Khatana C (2023) and Sharma, R., 2023. Mushroom and silk sericin extract mediated ZnO nanoparticles for removal of organic pollutants and microorganisms. S Afr J Bot 153:370–381
3. Bhatia N, Kumari A, Thakur N, Sharma G, Singh RR, Sharma R (2022) Phytochemically stabilized chitosan encapsulated Cu and Ag nanocomposites to remove cefuroxime axetil and pathogens from the environment. Int J Biol Macromol 212:451–464
4. Alavi M, Rai M (2019) Recent advances in antibacterial applications of metal nanoparticles (MNPs) and metal nanocomposites (MNCs) against multidrug-resistant (MDR) bacteria. Expert Rev Anti Infect Ther 17(6):419–428. https://doi.org/10.1080/14787210.2019.1614914
5. Rajamohan R, Raorane CJ, Kim SC, Ashokkumar S, Lee YR (2023) Novel microwave synthesis of copper oxide nanoparticles and appraisal of the antibacterial application. Micromachines 14(2):456. https://doi.org/10.3390/mi14020456
6. Rajamohan R, Lee YR (2023) Microwave-assisted synthesis of copper oxide nanoparticles by apple peel extract and efficient catalytic reduction on methylene blue and crystal violet. J Mol Struct 1276:134803. https://doi.org/10.1016/j.molstruc.2022.134803
7. Arya A, Gupta K, Chundawat TS, Vaya D (2018) Biogenic synthesis of copper and silver nanoparticles using green alga Botryococcus braunii and its antimicrobial activity. Bioinorg Chem Appl 2018:7879403. https://doi.org/10.1155/2018/7879403
8. Asghar MA, Asghar MA (2020) Green synthesized and characterized copper nanoparticles using various new plants extracts aggravate microbial cell membrane damage after interaction with lipopolysaccharide. Int J Biol Macromol 160:1168–1176. https://doi.org/10.1016/j.ijbiomac.2020.05.198
9. Asghari B, Mafakheri S, Zarrabi M, Erdem S, Orhan I, Bahadori M (2019) Therapeutic target enzymes inhibitory potential, antioxidant activity, and rosmarinic acid content of Echium amoenum. S Afr J Bot 120:191–197. https://doi.org/10.1016/j.sajb.2018.05.017
10. Bale VK, Katreddi HR (2022) Green synthesis, characterization and antimicrobial activity of nanosized Cuprous Oxide fabricated using aqueous extracts of Allium cepa and Raphanus sativus. Int J Nano Dimens 13(2):214–226. https://doi.org/10.22034/IJND.2022.687833
11. Bekhradnia S, Ebrahimzadeh MA (2016) Antioxidant activity of Echium amoenum. Rev Chim J 67(2):223–226
12. Chand Mali S, Dhaka A, Sharma S, Trivedi R (2023) Review on biogenic synthesis of copper nanoparticles and its potential applications. Inorg Chem Commun 149:110448. https://doi.org/10.1016/j.inoche.2023.110448
13 Chandraker SK, Lal M, Ghosh MK, Tiwari V, Ghorai TK, Shukla R (2020) Green synthesis of copper nanoparticles using leaf extract of Ageratum houstonianum Mill. and study of their photocatalytic and antibacterial activities. Nano Exp 1(1):010033. https://doi.org/10.1088/2632-959X/ab8e99
14. Prakash V, Kumari A, Kaur H, Kumar M, Gupta S, Bala R (2021) Green synthesis, characterization and antimicrobial activities of copper nanoparticles from the rhizomes extract of picrorhiza kurroa. Pharm Nanotechnol 9(4):298–306
15. Din MI, Arshad F, Hussain Z, Mukhtar M (2017) Green adeptness in the synthesis and stabilization of copper nanoparticles: catalytic, antibacterial, cytotoxicity, and antioxidant activities. Nanoscale Res Lett 12:1–15. https://doi.org/10.1186/s11671-017-2399-8
16. Erdenechimeg C, Guiqide A, Dejidmaa B, Chimedragchaa C, Purevsuren S (2017) Total phenolic, flavonoid, alkaloid and iridoid content and preventive effect of Lider-7-tang on lipopolysaccharide-induced acute lung injury in rats. Braz J Med Biol Res 50:e5916. https://doi.org/10.1590/1414-431X20175916
17. Ghasemi P, Shafiee G, Ziamajidi N, Abbasalipourkabir R (2022) Copper nanoparticles induce apoptosis and oxidative stress in SW480 human colon cancer cell line. Biol Trace Elem Res 157:1–9. https://doi.org/10.1007/s12011-022-03458-2
18. Ghosh MK, Sahu S, Gupta I, Ghorai TK (2020) Green synthesis of copper nanoparticles from an extract of Jatropha curcas leaves: characterization, optical properties, CT-DNA binding and photocatalytic activity. RSC Adv 10(37):22027–22035. https://doi.org/10.1039/D0RA03186K
19. Gu J, Aidy A, Goorani S (2022) Anti-human lung adenocarcinoma, cytotoxicity, and antioxidant potentials of copper nanoparticles green-synthesized by Calendula officinalis. J Exp Nanosci 17(1):285–296. https://doi.org/10.1080/17458080.2022.2066082
20. Gul R, Jan SU, Faridullah S, Sherani S, Jahan N (2017) Preliminary phytochemical screening, quantitative analysis of alkaloids, and antioxidant activity of crude plant extracts from Ephedra intermedia indigenous to Balochistan. Sci World J 2017:5873648. https://doi.org/10.1155/2017/5873648
21. Joseph AT, Prakash P, Narvi S (2016). Phytofabrication and characterization of copper nanoparticles using Allium sativum and its antibacterial activity. Int J Sci, Eng Technol 4:463-472. 10.2348. ijset03160463
22. Kefi S, Essid R, Mkadmini K, Kefi A, Haddada FM, Tabbene O, Limam F (2018) Phytochemical investigation and biological activities of Echium arenarium (Guss) extracts. Microb Pathog 118:202–210. https://doi.org/10.1016/j.micpath.2018.02.050
23. Kumar H, Bhardwaj K, Nepovimova E, Kuča K, Singh Dhanjal D, Bhardwaj S, Bhatia SK, Verma R, Kumar D (2020) Antioxidant functionalized nanoparticles: a combat against oxidative stress. Nanomaterials 10(7):1334. https://doi.org/10.3390/nano10071334
24. Kumar NH, Andia JD, Manjunatha S, Murali M, Amruthesh K, Jagannath S (2019) Antimitotic and DNA-binding potential of biosynthesized ZnO-NPs from leaf extract of Justicia wynaadensis (Nees) Heyne-A medicinal herb. Biocatal Agric Biotechnol 18:101024. https://doi.org/10.1016/j.bcab.2019.101024
25. Latif M, Abbas S, Kormin F, Mustafa M (2019) Green synthesis of plant-mediated metal nanoparticles: the role of polyphenols. Asian J Pharm Clin Res 12(7):75–84. https://doi.org/10.22159/ajpcr.2019.v12i7.33211
26. Lv Q, Zhang B, Xing X, Zhao Y, Cai R, Wang W, Gu Q (2018) Biosynthesis of copper nanoparticles using Shewanella loihica PV-4 with antibacterial activity: novel approach and mechanisms investigation. J Hazard Mater 347:141–149. https://doi.org/10.1016/j.jhazmat.2017.12.070
27. Marzban A, Mirzaei SZ, Karkhane M, Ghotekar SK, Danesh A (2022) Biogenesis of copper nanoparticles assisted with seaweed polysaccharide with antibacterial and antibiofilm properties against methicillin-resistant Staphylococcus aureus. J Drug Deliv Sci Technol 74:103499. https://doi.org/10.1016/j.jddst.2022.103499
28. Mehran M, Masoum S, Memarzadeh M (2020) Improvement of thermal stability and antioxidant activity of anthocyanins of Echium amoenum petal using maltodextrin/modified starch combination as wall material. Int J Biol Macromol 148:768–776. https://doi.org/10.1016/j.ijbiomac.2020.01.197
29. Menazea A, Ahmed M (2020) Silver and copper oxide nanoparticles-decorated graphene oxide via pulsed laser ablation technique: preparation, characterization, and photoactivated antibacterial activity. Nano-Struct Nano-Objects 22:100464. https://doi.org/10.1016/j.nanoso.2020.100464

30 Murthy H, Desalegn T, Kassa M, Abebe B, Assefa T (2020) Synthesis of green copper nanoparticles using medicinal plant hagenia abyssinica (Brace) JF. Gmel. leaf extract: Antimicrobial properties. J Nanomater 2020:3924081. https://doi.org/10.1155/2020/3924081
31. Nethravathi P, Kumar MP, Suresh D, Lingaraju K, Rajanaika H, Nagabhushana H, Sharma S (2015) Tinospora cordifolia mediated facile green synthesis of cupric oxide nanoparticles and their photocatalytic, antioxidant and antibacterial properties. Mater Sci Semicond Process 33:81–88. https://doi.org/10.1016/j.mssp.2015.01.034
32. Poonguzhali G, Noorjahan C, Keerthana S (2022) Biosynthesis of copper nanoparticles using chitosan extracted from prawn shells, characterization and antimicrobial activity. Asian J Biol Life Sci 11(3):737. https://doi.org/10.5530/ajbls.2022.11.98
33. Punniyakotti P, Panneerselvam P, Perumal D, Aruliah R, Angaiah S (2020) Anti-bacterial and anti-biofilm properties of green synthesized copper nanoparticles from Cardiospermum halicacabum leaf extract. Bioprocess Biosyst Eng 43(9):1649–1657. https://doi.org/10.1007/s00449-020-02357-x
34. Rajeshkumar S, Menon S, Kumar SV, Tambuwala MM, Bakshi HA, Mehta M, Satija S, Gupta G, Chellappan DK, Thangavelu L (2019) Antibacterial and antioxidant potential of biosynthesized copper nanoparticles mediated through Cissus arnotiana plant extract. J Photochem Photobiol B: Biology 197:111531. https://doi.org/10.1016/j.jphotobiol.2019.111531
35. Ramzan M, Obodo RM, Mukhtar S, Ilyas S, Aziz F, Thovhogi N (2021) Green synthesis of copper oxide nanoparticles using Cedrus deodara aqueous extract for antibacterial activity. Mater Today: Proceedings 36:576–581. https://doi.org/10.1016/j.matpr.2020.05.472
36. Rehana D, Mahendiran D, Kumar RS, Rahiman AK (2017) Evaluation of antioxidant and anticancer activity of copper oxide nanoparticles synthesized using medicinally important plant extracts. Biomed Pharmacother 89:1067–1077. https://doi.org/10.1016/j.biopha.2017.02.101
37. Reyes-Torres MA, Mendoza-Mendoza E, Miranda-Hernández ÁM, Pérez-Díaz MA, López-Carrizales M, Peralta-Rodríguez RD, Sánchez-Sánchez R, Martinez-Gutierrez F (2019) Synthesis of CuO and ZnO nanoparticles by a novel green route: antimicrobial activity, cytotoxic effects and their synergism with ampicillin. Ceram Int 45(18):24461–24468. https://doi.org/10.1016/j.ceramint.2019.08.171
38. Rezaie AB, Montazer M, Rad MM (2017) Biosynthesis of nano cupric oxide on cotton using Seidlitzia rosmarinus ashes utilizing bio, photo, acid sensing and leaching properties. Carbohyd Polym 177:1–12. https://doi.org/10.1016/j.carbpol.2017.08.053
39. Roszczenko P, Szewczyk OK, Czarnomysy R, Bielawski K, Bielawska A (2022) Biosynthesized gold, silver, palladium, platinum, copper, and other transition metal nanoparticles. Pharmaceutics 14(11):2286. https://doi.org/10.3390/pharmaceutics14112286
40. Santha A, Varghese R, Joy Prabu H, Johnson I, Magimai Antoni Raj D, John Sundaram S (2021) Production of sustainable biofuel from biogenic waste using CuO nanoparticles as heterogeneous catalyst. Mater Today: Proceedings 36:447–452. https://doi.org/10.1016/j.matpr.2020.05.069
41. Shi L-B, Tang P-F, Zhang W, Zhao Y-P, Zhang L-C, Zhang H (2017) Green synthesis of CuO nanoparticles using Cassia auriculata leaf extract and in vitro evaluation of their biocompatibility with rheumatoid arthritis macrophages (RAW 264.7). Trop J Pharm Res 16(1):185–192. https://doi.org/10.4314/tjpr.v16i1.25
42. Siddiquee MA, Mud P, Kamli MR, Malik MA, Mehdi SH, Imtiyaz K, Rizvi MMA, Rajor HK, Patel R (2021) Biogenic synthesis, in-vitro cytotoxicity, esterase activity and interaction studies of copper oxide nanoparticles with lysozyme. J Market Res 13:2066–2077. https://doi.org/10.1016/j.jmrt.2021.05.078
43. Singh A, Singh N, Hussain I, Singh H (2017) Effect of biologically synthesized copper oxide nanoparticles on metabolism and antioxidant activity to the crop plants Solanum lycopersicum and Brassica oleracea var. botrytis. J Biotechnol 262:11–27. https://doi.org/10.1016/j.jbiotec.2017.09.016
44. Sohrabnezhad S, Pourahmad A, Salavatiyan T (2016) CuO–MMT nanocomposite: effective photocatalyst for the discoloration of methylene blue in the absence of H2O2. Appl Phys A 122(2):111. https://doi.org/10.1007/s00339-016-9645-2
45. Venkateswara Rao A, Ashok B, Uma Mahesh M, Venkata Subbareddy G, Chandra Sekhar V, Venkata Ramanamurthy G, Varada Rajulu A (2019) Antibacterial cotton fabrics with in situ generated silver and copper bimetallic nanoparticles using red sanders powder extract as reducing agent. Int J Polym Anal Charact 24(4):346–354. https://doi.org/10.1080/1023666X.2019.1598631
46. Vorobyev S, Likhatski M, Romanchenko A, Maksimov N, Zharkov S, Krylov A, Mikhlin Y (2018) Colloidal and deposited products of the interaction of tetrachloroauric acid with hydrogen selenide and hydrogen sulfide in aqueous solutions. Minerals 8(11):492. https://doi.org/10.3390/min8110492
47. Wang P, Zheng X, Wu X, Wei X, Zhou L (2012) Preparation and characterization of CuO nanoparticles encapsulated in mesoporous Silica. Microporous Mesoporous Mater 149(1):181–185. https://doi.org/10.1016/j.micromeso.2011.07.002
48. Yugandhar P, Vasavi T, Jayavardhana Rao Y, Uma Maheswari Devi P, Narasimha G, Savithramma N (2018) Cost effective, green synthesis of copper oxide nanoparticles using fruit extract of Syzygium alternifolium (Wt.) Walp., Characterization and Evaluation of Antiviral Activity. J Clust Sci 29(4):743–755. https://doi.org/10.1007/s10876-018-1395-1